

# Interpretable Robotic Manipulation from Language

Boyuan Zheng<sup>a</sup>, Jianlong Zhou<sup>a</sup> and Fang Chen<sup>a</sup>

<sup>a</sup>University of Technology Sydney

**Abstract.** Humans naturally employ linguistic instructions to convey knowledge, a process that proves significantly more complex for machines, especially within the context of multitask robotic manipulation environments. Natural language, moreover, serves as the primary medium through which humans acquire new knowledge, presenting a potentially intuitive bridge for translating concepts understandable by humans into formats that can be learned by machines. In pursuit of facilitating this integration, we introduce an explainable behavior cloning agent, named Ex-PERACT, specifically designed for manipulation tasks. This agent is distinguished by its hierarchical structure, which incorporates natural language to enhance the learning process. At the top level, the model is tasked with learning a discrete skill code, while at the bottom level, the policy network translates the problem into a voxelized grid and maps the discretized actions to voxel grids. We evaluate our method across eight challenging manipulation tasks utilizing the RLbench benchmark, demonstrating that Ex-PERACT not only achieves competitive policy performance but also effectively bridges the gap between human instructions and machine execution in complex environments. Code, data, and supplementary materials are publicly available at <https://anonymous.4open.science/r/ExPERACT>.

## 1 Introduction

The exploration of sequential decision-making within the realm of artificial intelligence (AI) is a pivotal research focus, bearing substantial implications for applications such as autonomous driving, gaming strategy, and humanoid robotics [23, 22, 36]. Central to this pursuit is imitation learning (IL), which entails learning from demonstrations and emerges as a promising primary approach to effectively address the challenges inherent in sequential decision-making. To enhance the capabilities of intelligent agents, research communities have integrated various forms of auxiliary information, including human preferences, task-specific parameters, and the expertise level of experts [3, 19, 1]. Notably, advancements in large language models have established natural language as a preferred method among researchers, owing to its intuitiveness and provision of a more universally applicable means for instructing agents. Diverse methodologies proposed in studies such as [30, 25, 39] are aimed at training single-task agents, utilizing the conventional state-action pair as input and supplementing it with natural language as auxiliary information.

As machine learning techniques progress, there has been a gradual enhancement in the performance of intelligent agents across single tasks, instilling anticipation among researchers for adept multitask domain performance. These intelligent agents are designed to acquire knowledge from offline demonstrations spanning various tasks and appropriately interact with the environment during testing time. The

integration of natural language holds promise in strengthening the interconnections between tasks, thereby fostering an enhanced ability to reuse acquired skills across similar tasks. Studies such as PERACT [29] and BC-Z [14] exemplify how the incorporation of natural language into multitask models significantly influences task success rates, underscoring its potential impact in advancing the field.

However, training a language-conditioned multitask model poses significant challenges. Firstly, language instructions often fail to fully elucidate tasks due to inherent limitations in common-sense reasoning. For instance, instructions like “Open drawer” may overlook crucial steps such as targeting and gripping the drawer handle, thereby hindering the summarization and reusability of implicit sub-tasks for comparable activities. Moreover, the inherently abstract nature of language provides limited information about subtask divisions and lacks ground truth for potential skills, rendering the learning process unsupervised. Furthermore, task instructions may vary among individuals, introducing complexities into the training of multitask models due to the diversity in expression. Additionally, while natural language provides a means for humans to probe the model and enhance interpretability, this aspect has garnered limited attention in multitask model research.

To address the aforementioned challenges and delve deeper into explainability, we propose a novel method named Ex-PerAct. This approach employs a hierarchical structure and integrates multitask imitation learning to acquire reusable skills from language-conditioned offline demonstrations. Ex-PerAct comprises two transformer-based models in sequence. The top-level model condenses skills from diverse tasks into discrete skill codes, providing a comprehensive summary of segmented demonstration snippets. This model acts as a vital bridge connecting human-understandable natural language to digital skill vectors, thereby facilitating the reuse of condensed skills in analogous tasks. To cluster these skill vectors in an unsupervised manner, we employ Vector Quantization (VQ) [31]. As for the bottom-level model, we leverage the state-of-the-art PerAct [29], a multitask Behavior Cloning agent renowned for its competitive performance across a wide array of manipulation tasks. PerAct represents observations and actions as 3D voxels rather than 2D image pixels, contributing to its superior capabilities. We conduct experiments on eight manipulation tasks in the challenging benchmark RLbench [12] with multiple baselines and ablations. The results demonstrate that Ex-PERACT achieves better policy performance in almost all tasks while providing an interpretable way for humans to probe the relationship between language instructions and the agent’s decision-making process.

We highlight the primary contributions of this paper as follows:

- We present Ex-PerAct, a hierarchical imitation learning method that effectively integrates diverse modalities, including 3D voxels

and language instructions, thereby achieving competitive performance across tasks.

- Our approach showcases the capacity of Ex-PerAct to extract reusable skills across tasks, offering significant advantages in the realm of multitask robotic manipulation.
- Ex-PerAct forges a crucial link between human-understandable natural language and machine-usable vectors, augmenting interpretability across behavioral patterns, and language instructions.

## 2 Related Work

### 2.1 Language-conditioned imitation learning in robotic manipulation

The integration of natural language into the training of intelligent agents has emerged as a prominent trend, with roots extending beyond recent years. Chen and Mooney introduced a framework facilitating the learning of a semantic parser, aligning instructions with the world state in navigation tasks [4]. The rise of transformer-based models has ushered in a proliferation of language-conditioned datasets in contemporary research. Pioneering investigations such as [14, 16, 20, 29, 8] seamlessly incorporate this modality with imitation learning, tackling more intricate continuous manipulation tasks compared to earlier studies.

Noteworthy among recent advancements is the work by Nair et al., who annotated an offline dataset with crowd-sourced natural language labels. They introduced LOReL, a method that recovers a language-conditioned reward function represented by a simple classifier, specifically tailored for integration into multi-task reinforcement learning [21]. This annotated dataset has since played a pivotal role in numerous subsequent investigations focusing on language-conditioned robotic manipulation, exemplified by [7]. Concurrently, Shridhar et al. introduced CLIPORT, a method leveraging natural language to achieve commendable performance levels in both simulated and real-world domains [28].

Despite the breadth of literature in this domain, research into the potential enhancement of explainability through the incorporation of natural language remains relatively limited. LISA, as proposed by Garg et al., employs a hierarchical imitation learning framework that learns interpretable skill abstractions from a language-conditioned dataset using state-of-the-art transformer-based models, elucidating the correlation between natural language and acquired skills [7]. However, LISA introduces additional parameters such as horizon, and the model’s performance is heavily reliant on these parameters. Moreover, its evaluation in multitasks related to manipulation is notably constrained, and its performance in established benchmarks like RLBench is also limited.

### 2.2 Hierarchical imitation learning

The hierarchical structure has emerged as a beneficial paradigm in numerous studies on imitation learning, offering various advantages derived from its ability to harness benefits from different models. One notable advantage is exemplified by Le et al., who introduced a hierarchical framework encompassing both imitation learning (IL) and reinforcement learning (RL). Their study showcased that employing different combinations of IL and RL at distinct levels could notably mitigate expert effort and exploration costs, rendering their proposed framework more label-efficient compared to standard IL [17].

Furthermore, hierarchical frameworks excel in facilitating the learning of separate sub-task policies for complex tasks, leading to

performance enhancements. Hierarchical option frameworks represent a prevalent approach for learning sub-task policies, categorized into those trained with ground truth option labels [37, 18] and those utilizing alternative forms of supervision [27, 32, 7]. For instance, FIST, proposed by Hakhamaneshi et al., falls under the former category, employing an inverse dynamic model to extract generalizable skills offline and achieving competitive performance in long-horizon tasks under few-shot settings [9]. Conversely, in the latter category, Zhang and Paschalidis explored the Expectation-Maximization approach to hierarchical IL from a theoretical standpoint, devising the first convergence guarantee algorithm that solely observes primitive state-action pairs [38].

In addition to performance improvements, hierarchical IL also enhances explainability, as will be further elucidated in the subsequent subsection. Broadly, the high-level options serve as a bridge between human-understandable knowledge and the model’s performance, acting as a bottleneck to facilitate clearer comprehension. Our work similarly follows this principle but emphasizes explainability regarding language over the input demonstrations.

### 2.3 Explainable imitation learning

The exploration of the explainability of IL methods has gained traction in recent years, with a notable shift towards enhancing interpretability for non-technical audiences. Early research, proposed in [19], aimed to learn interpretable and meaningful representations to infer the latent structure of input demonstrations, albeit without delving deeply into improving explainability for non-technical users. Subsequently, in 2020, Pan et al. introduced xGAIL, claiming it as the first explainable GAIL framework. As explainable AI gains prevalence, an increasing number of studies are emerging that combine eXplainable AI (XAI) with IL methodologies.

Leech proposed an intrinsically interpretable IL method that leverages a hierarchical learning framework and integrates IL with logical automata. This approach represents problems as compact finite state automata with human-interpretable logic states [18]. Similarly, Bewley et al. (2020) introduced an explainable IL method employing interpretable models, wherein they model the behavior policy of a trained black-box agent using a decision tree generated from analyzing its input-output statistics [2].

In addition to intrinsically interpretable approaches, post-hoc explanation methodologies are prevalent in the research community [34, 7, 15]. Zhang et al. (2021) utilized a hierarchical framework to achieve post-hoc explanation, decomposing complex tasks and elucidating the model’s decision-making process and causes of failure [37]. Wang et al. proposed subgoal-conditioned hierarchical IL to emulate doctors’ behavior, providing more explainable post-hoc recommendations in the dynamic treatment recommendation domain [32]. However, these methods seldom investigate natural language as the primary communication medium between individuals. With the prevalence of transformer-based models and their capacity to address sequential data such as language, natural language is gradually being incorporated into the training process. This integration should serve as a bottleneck to enhance explainability, as it enables a more intuitive interaction between humans and machines.

## 3 Approach

Our approach, Ex-PERACT, introduces an explainable hierarchical agent for 6-DOF manipulation tasks. It adopts a behavior cloning approach, training on a language-conditioned offline dataset. The core

concept involves extracting discrete skill codes to bridge natural language instructions with observation at a higher level, while simultaneously learning a policy network from the extracted skill code, language embeddings, and observation-action pair at a lower level. The skill codes is learned unsupervisedly and enhance explainability with respect to the natural language and multitask learning. Additionally, the design incorporates 3D voxel reconstruction inherited from PERACT, which significantly improves learning efficiency compared to conventional 2D image-action mapping.

We begin by presenting the preliminary knowledge and our problem formulation in Section 3.1. Subsequently, Section 3.2 delves into the framework of Ex-PERACT, providing a comprehensive introduction to the models. Finally, Section 3.3 elucidates further implementation details.

### 3.1 Problem setting

We conceptualize our problem as multitask, where each task  $T_i$  can be regarded as an individual Markov Decision Process (MDP), characterized by the property that the next state  $s_{t+1}$  is solely determined by the current state  $s_t$  at any time  $t$ . We assume access to an offline dataset  $D$  generated by an optimal policy, comprising  $m$  expert demonstration trajectories from a wide range of tasks, denoted as  $D = \tau_1, \tau_2, \dots, \tau_m$ . Each trajectory  $\tau$  comprises a sequence of state-action pairs accompanied by a natural language instruction, structured as  $\tau_i = l^i, (s_1^i, a_1^i), (s_2^i, a_2^i), \dots, (s_n^i, a_n^i)$ . Each task  $T_i$  can be further decomposed into multiple snippets of various lengths, each representing simpler sub-goals. For instance, a task such as "Take the steak off the grill" may decompose into sub-goals like "Moving the gripper to target the steak", "Picking up the steak", and "Placing the steak at the destination". However, such explicit instructions are uncommon in daily life, often leading individuals to overlook common sense steps. Our method, Ex-PERACT, aims to categorize these implicit steps at the top-level model from the offline dataset, and to simplify the problem, we assume the each snippet only encodes one sub-goal.

In line with previous research, we adopt the approach introduced by James et al. for trajectory decomposition [13]. A simple heuristic is designed to extract keyframes from demonstration: a timestep is assigned as a keyframe if the joint velocity is close to zero or if the gripper's status changes (from open to close, and vice versa). The actions of these extracted keyframes are also utilized as macro-actions during training, enhancing robustness and mitigating the effects of randomness and noise inherent in original continuous actions.

We employ PERACT's voxelization method to reconstruct 3D representations from RGB-D image observations [29]. This approach partitions a  $1.0m^3$  space into  $100^3$  voxel grids (See Figure 1). These discrete representations of observation and action facilitate reformulating the problem as a "next best action" classification problem [13], wherein the  $(x, y, z)$  location of the voxel grid corresponds to the coordination of the gripper's center, while the robotic arm's rotation is discretized similarly over three axes with a 5-degree resolution.

Despite decomposing trajectories into snippets of various lengths, the sub-goals or skills represented by these snippets remain unknown. Due to this lack of prior knowledge, we train the top-level model in an unsupervised manner, utilizing vector quantization to summarize skills into discrete skill codes.

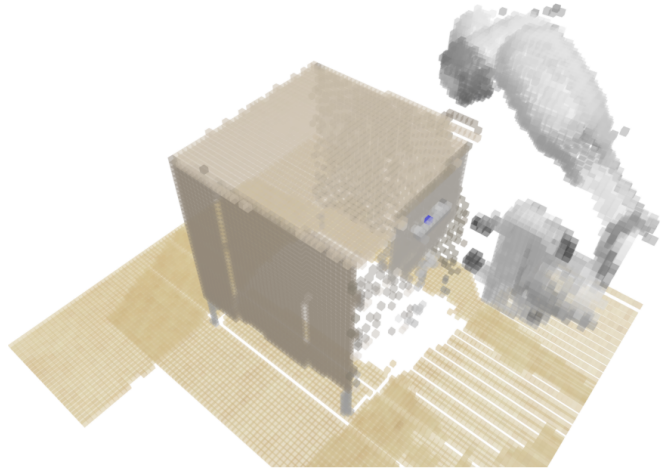


**Figure 1:** Illustration of Voxelization for the "Open Drawer" Task, adapted from [29]. RGB-D image inputs undergo transformation into  $(100,100,100)$  voxel grids, representing a cubic meter space.

### 3.2 Ex-PERACT

Ex-PERACT is a two-level hierarchical framework designed to process language instructions ( $\mathcal{L}$ ) and observations ( $\mathcal{O}$ ), yielding discretized actions comprising three aspects of behavior: coordination (also known as translation), quaternion rotation, and gripper state ( $\mathcal{A} = \mathcal{A}_{\text{coord}}, \mathcal{A}_{\text{rotation}}, \mathcal{A}_{\text{gripper}}$ ) (see Figure 2). Both levels of the model employ transformer-based architectures to handle sequential input. At the top level, a transformer model learns discrete skill codes from a single language instruction and a sequence of observations, represented as  $f(\mathcal{O}, \mathcal{L}) \mapsto \mathcal{C}$ . Meanwhile, the bottom level transformer learns a policy in a command-conditional behavior cloning manner, denoted as  $\pi(\mathcal{O}, \mathcal{C}, \mathcal{L}) \mapsto \mathcal{A}$ , akin to previous work [5]. Drawing inspiration from the promising results of CLIP in manipulation tasks reported in prior literature [33, 28, 8], Ex-PERACT also incorporates CLIP [24]. CLIP is renowned for its generalization capabilities and effectiveness in multimodal domains. The tokenizer and pre-trained model of CLIP are employed to tokenize and encode human-understandable language into language embeddings with dimensions of  $(77, 512)$ . Additionally, we fine-tune the language embeddings using a linear layer to further enhance their effectiveness.

The input observation consists of a set of observations, encompassing not only the observation at the current timestep but also those from both past and future keyframes. Each observation comprises RGB-D inputs from four cameras (front, left shoulder, right shoulder, and wrist). As the heuristically identified keyframes divide each demonstration into multiple snippets, at timestep  $t$ , history observations are randomly sampled within the same snippet. The skill code at timestep  $t$  is then obtained via majority vote from these history observations, ensuring consistency and robustness. Future keyframe observations are extracted from the remaining keyframes from timestep  $t$ . All these observations are chronologically ordered and fed into the top-level model as a sequence. Initially, we fuse and encode the RGB-D input of each observation using a Convolutional Neural Network (CNN). The encoded observation embeddings are then combined with positional embeddings obtained from the timestep indexes of the observations and concatenated with the language embeddings from the pre-trained CLIP model. This language-observation embeddings are inputted into a simple causal transformer with a single self-attention layer followed by a linear layer, generating continuous skill

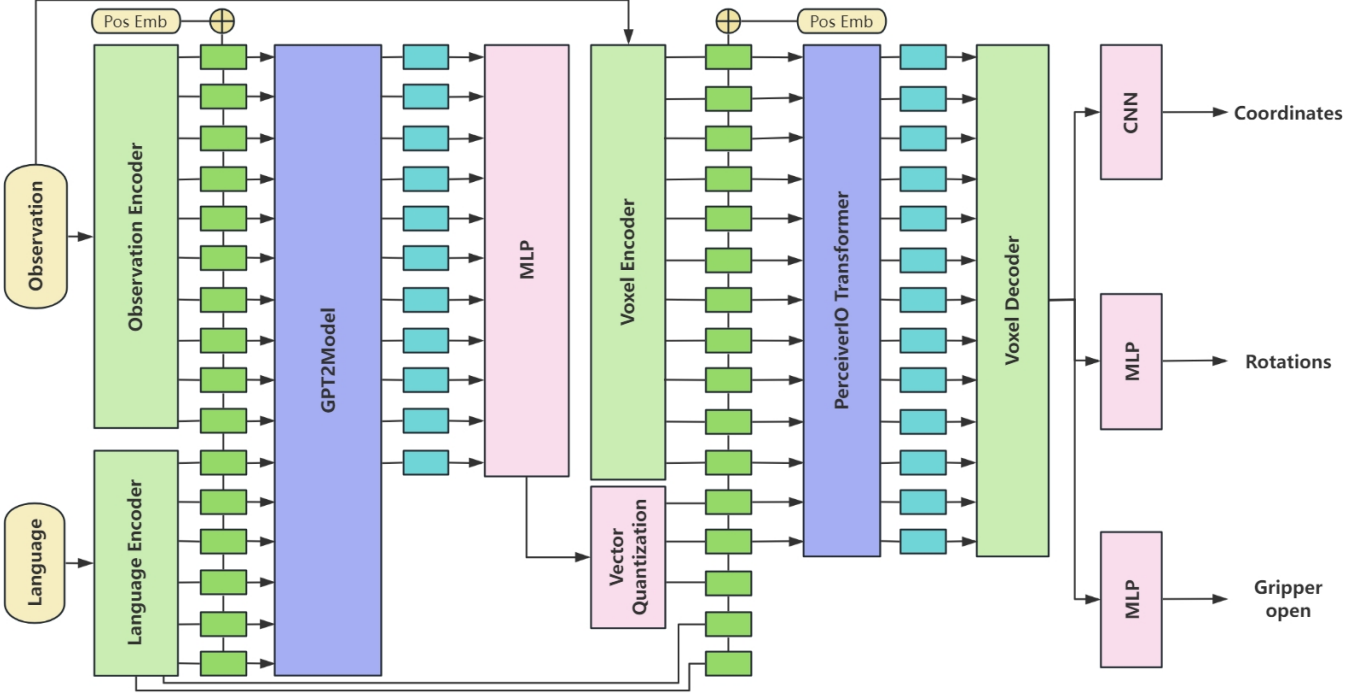


**Figure 2:** A diagram illustrating the Ex-PERACT framework. Ex-PERACT, a hierarchical model, aims to learn reusable skills to improve explainability and predict actions based on given observations. Language instructions are encoded using a pre-trained CLIP model, while observations are preprocessed into embeddings or voxels. The top-level model takes language embeddings and observation embeddings as input, producing discretized skill code estimates. Meanwhile, the bottom-level model receives voxel inputs, language embeddings, and discretized skill code estimates, generating action predictions from three perspectives.

code estimates for each observation in the input, i.e.,  $\hat{c}_t = f(o_t, l)$ , where  $o_t$  represents the individual observation at timestep  $t$ , and  $l$  denotes the language instruction of the task. Due to the lack of prior knowledge regarding the skill codes, we utilize vector quantization  $vg(\cdot)$  to cluster and discretize these learned continuous skill code estimates, yielding  $\tilde{c} = vg(\hat{c})$ .

We train Ex-PERACT end-to-end using the command-conditional behavior cloning paradigm. The standard command-conditional behavior cloning, as introduced in [5], can be represented by the following equation:

$$\text{minimize} \sum_i \mathcal{L}(\pi(o_i, c_i), a_i). \quad (1)$$

Since we lack prior knowledge of the skill codes, and they are learned unsupervisedly in the top-level model, we introduce vector quantization loss in Equation 1. Vector quantization loss is calculated as the mean squared error between the discretized skill code estimate and the continuous skill code. Additionally, considering the action decomposition into three categories, we independently calculate the cross-entropy loss for each type of action. Consequently, the objective of Ex-PERACT can be formulated as follows:

$$\begin{aligned} \text{minimize} \sum_i \mathcal{L}_{CE}(\pi_{coord}(o_i, c_i, l), a_i^{\text{coord}}) + \\ \mathcal{L}_{CE}(\pi_{rot}(o_i, c_i, l), a_i^{\text{rot}}) + \\ \mathcal{L}_{CE}(\pi_{grip}(o_i, c_i, l), a_i^{\text{grip}}) + \\ \mathcal{L}_{MSE}(f(o_i, l), \tilde{c}_i), \end{aligned} \quad (2)$$

where the last term can be directly obtained from the top-level model, and the first three terms are calculated after each iteration.

To obtain various types of actions, we employ another transformer-based model to predict coordinates, rotation, and gripper state separately. At timestep  $t$ , the top-level model takes the observation set and language instruction as input, while at the bottom level, the same observation set and language embeddings together with obtained skill code estimates are used as input. The observations are reconstructed into voxels  $v$  with a shape of  $(100, 100, 100)$  using a similar approach as described in both [13] and [29]. These  $100^3$  voxel grids are then split and flattened into sequences with a length of  $(100/5)^3 = 8000$  using a 3D convolutional layer with kernel and stride size set to five. The flattened voxel sequence is subsequently concatenated with the extracted skill code estimate and language embeddings, and then fed into a six-layer self-attention model. Considering the potential memory limitations when processing long sequences on commodity GPUs, we adopt the Perceiver Transformer  $pt(\cdot)$  with 512 latents of dimension 512 [10]. The Perceiver Transformer allows for projection from a long sequence to a much shorter latent space and then projects the final output latent back to the original input size. The features of each voxel grid are obtained from the output of the Perceiver Transformer after decoding, which are then utilized to predict coordinates using a 3D CNN or rotation and gripper status using a Multilayer Perceptron (MLP). Specifically:

$$\begin{aligned} \hat{a}_t^{\text{coord}} &= \pi_{coord}(pt(o_t, c_t, l)) \\ \hat{a}_t^{\text{rot}} &= \pi_{rot}(pt(o_t, c_t, l)) \\ \hat{a}_t^{\text{grip}} &= \pi_{grip}(pt(o_t, c_t, l)). \end{aligned} \quad (3)$$

**Table 1:** Multitask performance comparison across state-of-the-art methods. Values represent mean success rate (%) obtained from 25 evaluation episodes per task with the best ones bolded.

| method                                  | open drawer | meat off grill | slide block | turn tap  | close jar | stack blocks | screw bulb | push buttons |
|---|-------------|----------------|-------------|-----------|-----------|--------------|------------|--------------|
| BC (CNN)                                | 4           | 0              | 4           | 20        | 0         | 0            | 0          | 4            |
| BC (ViT)                                | 16          | 0              | 8           | 24        | 0         | 0            | 0          | 16           |
| LISA                                    | 8           | 0              | 4           | 28        | 0         | 0            | 0          | 20           |
| C2FARM-BC                               | 28          | 40             | 12          | 60        | 28        | 4            | 12         | 88           |
| Ex-PERACT (Obs only)                    | 20          | 40             | 8           | 36        | 16        | 0            | 0          | 60           |
| Ex-PERACT (Obs + skill code)            | 28          | 56             | 16          | 48        | 16        | 4            | 20         | 72           |
| Ex-PERACT (Obs + Lang, which is PERACT) | 64          | 68             | 32          | 60        | 28        | <b>8</b>     | 28         | 56           |
| Ex-PERACT (single Lang)                 | <b>76</b>   | <b>80</b>      | <b>44</b>   | 60        | 32        | 0            | <b>36</b>  | <b>92</b>    |
| Ex-PERACT (multi Lang)                  | 72          | <b>80</b>      | <b>44</b>   | <b>88</b> | <b>40</b> | <b>8</b>     | 24         | 88           |

### 3.3 Implementation

The Ex-PERACT framework is hierarchical in nature, and we employ the single LAMB optimizer [35] to update parameters from both the top and bottom-level models. To facilitate end-to-end training within a framework containing non-differentiable components like VQ, we utilize a technique known as the straight-through estimator. This method directly propagates gradients from the decoder to the encoder. Given that actions are discretized, cross-entropy losses for three types of actions are computed by comparing the action estimates encoded with ground truth one-hot encoding. Specifically, for rotation, the loss is calculated under the 3D Euler angle coordinate setting, with the final rotation action reconstructed from the Euler angles into a quaternion. Demonstration inputs are obtained with the assistance of a motion planner in RL Bench, with each demonstration sourced from a different variance number. Since observation inputs for specific timesteps consist of observation sets, we set the sample frequency and batch size to 10 and 1, respectively, to ensure efficient disk and memory usage on commodity devices. Observations reveal significant variations in demonstration length across tasks, ranging from approximately 100 to over 400 timesteps. Additionally, the number of identified keyframes exhibits considerable deviation, ranging from 2 to around 20. To maintain a similar sample frequency for each sample, we set the sampling weights as the sum of the total number of observations for each task and the size of the observation set. In the bottom-level model, we implement data augmentation prior to voxelization.

## 4 Result

In this section, we present our experimental setup and findings. We assess Ex-PERACT’s performance using RL Bench manipulation tasks, comparing its multitask capabilities against those of other state-of-the-art methods. Additionally, we analyze the explainability provided by the hierarchical framework.

### 4.1 Experiment setup

Ex-PERACT is evaluated within the RL Bench simulation platform, utilizing a GPU NVIDIA Quadro RTX 5000 for computations. RL Bench operates on CoppeliaSim/V-REP [26] and PyRep [11] interfaces, featuring a Franka Emika Panda robot arm with six degrees of freedom (DOF). This platform provides crucial data such as joint velocities, angles, and forces, alongside four  $128 \times 128$  RGB-D images captured from different camera perspectives. Diverse manipulation tasks are designed, ensuring variability in task execution and accompanying language summaries. To manage memory usage effectively,

all samples are stored on disk. We select eight tasks spanning from opening a drawer to screwing in a light bulb, with ten demonstrations collected for each task. For comparison, we evaluate several state-of-the-art imitation learning (IL) methods as baselines. Baseline agents include BC with image encoder CNN and Vision Transformer (ViT) [6], LISA [7], C2FARM-BC [13], and PERACT [29]. BC and LISA are image-to-action agents mapping observed RGB-D images to eight-dimensional actions. In contrast, C2FARM-BC, PERACT, and Ex-PERACT are voxel-to-action agents, reconstructing the 3D space and discretizing the problem as a classification task. While C2FARM-BC adopts a two-level voxelization allowing zoom-in operations for higher resolution ( $0.47cm^3$ ), PERACT and Ex-PERACT employ a voxel resolution of  $1cm^3$ . Each agent interacts with the test environment via a motion planner, and the mean success rate is computed from 25 episodes per task ( $8 \times 25 = 200$  total episodes evaluated). Success is defined as reaching the goal state within 25 steps, while episodes encountering issues such as exceeding the maximum steps, encountering an invalid path, or having the target outside the workspace are deemed failures.

### 4.2 Policy performance

Table 1 presents the average success rates of state-of-the-art methods and our method Ex-PERACT. The first three methods are image-based BC agents, while the remaining methods employ a 3D representation. The “single lang” Ex-PERACT denotes that the language instructions are in a consistent format for a specific task, whereas the “multi-lang” Ex-PERACT indicates variable instruction formats across batches. For example, in the task “open drawer”, a consistent instruction would be “open the top/middle/bottom drawer”; under the “multi-lang” condition, the instructions could vary randomly, including “open the top/middle/bottom drawer”, “grip the top/middle/bottom handle and pull the top/middle/bottom drawer open”, or “slide the top/middle/bottom drawer open”. All methods receive the same set of 80 demonstrations ( $8 \times 10 = 80$ ) as input. Analysis of Table 1 reveals that image-based methods demonstrate poor performance across all tasks, whereas those utilizing 3D representation consistently outperform them. With only 10 demonstrations available per task, image-based agents face significant challenges across all eight tasks. This finding underscores the formidable task of learning hand-eye coordination from scratch, given its inherent demands for time and data. Furthermore, this comparison supports our contention that 3D voxelization offers enhanced data efficiency. Among methods employing 3D representation, our approach, Ex-PERACT, which integrates various language inputs, consistently demonstrates superior policy performance. It surpasses PERACT by an average improvement of 29.07% (the third row from the bot-



tom) and achieves a 63.23% better average performance compared to C2FARM.

We observe that C2FARM, PERACT, and Ex-PERACT perform better in tasks like “open drawer”, “meat off grill”, and “turn tap”, which have relatively fewer variations, namely 3 (top/middle/bottom), 2 (steak/drumstick), and 2 (left/right), respectively. This pattern indicates that the performance of BC agents is highly dependent on the number of variations in a task. Moreover, all evaluated methods show limited success in the task “stack blocks” (with a maximum of 60 variations). In addition to the influence of highest variation number, we think the principal challenge lies in the degree of freedom of the manipulable objects. The more states these objects can reach, the more challenging it is for BC agents to learn, as minor errors can be magnified during the manipulation of multiple objects. For example, although Ex-PERACT can successfully stack the first block, any minor misalignment in the location or rotation of the first blocks degrades the performance of subsequent actions. The impact of such errors becomes even amplified as more blocks are stacked. This is likely a major contributing factor to the difficulties encountered in the “stack blocks” task, considering the promising performance in task “push buttons” while “push buttons also possesses a maximum 50 variation number.

We conducted an ablation study to investigate the impact of skill code availability, language, and their combination, as well as language diversity, on performance. The results of this analysis are presented in the fifth-to-last row of Table 1. Comparing Ex-PERACT with observation only to Ex-PERACT with both skill code and observation, we conclude that the inclusion of skill code provides useful information to enhance agent policy performance. In comparing Ex-PERACT with skill code to Ex-PERACT with language (PERACT), we observed that Ex-PERACT with language significantly outperforms Ex-PERACT with skill code. This finding contradicts the result in [7], where non-hierarchical Ex-PERACT with language performed worse than hierarchical Ex-PERACT with skill code. We believe the reason for this discrepancy is that the limited number of skills is inadequate to represent tasks with large varieties. This assertion is supported by the performance of Ex-PERACT with skill code, particularly in low variety tasks such as “meat off grill” and “turn tap”, where the agent performs relatively better than in tasks with greater variety. Additionally, comparing the performance between single-language Ex-PERACT and multi-language Ex-PERACT, the results indicate that the inclusion of diverse language instructions does not detract from the performance of Ex-PERACT.

### 4.3 Explainable skill representation

To evaluate the explainability of Ex-PERACT, we aggregated the input language instructions alongside the corresponding output skill codes into a dictionary. In this dictionary, each key represents a skill code generated by the Ex-PERACT system, while the corresponding value comprises a list of words extracted from the language instructions. Notably, common stop words such as “from”, “it”, and “to” were excluded from the list. The rationale behind this methodology is to leverage frequently occurring words to elucidate the learned skill codes. Following this compilation, we explored various visualization techniques to represent the human-understandable verbal meanings of the skill codes. Traditional methods, such as heat maps, are less intuitive due to the heterogeneous formats of language instructions and the potential inundation of words, resulting in a dense and overwhelming visualization. Consequently, we opted for a word cloud to enhance accessibility for less technically inclined audiences.

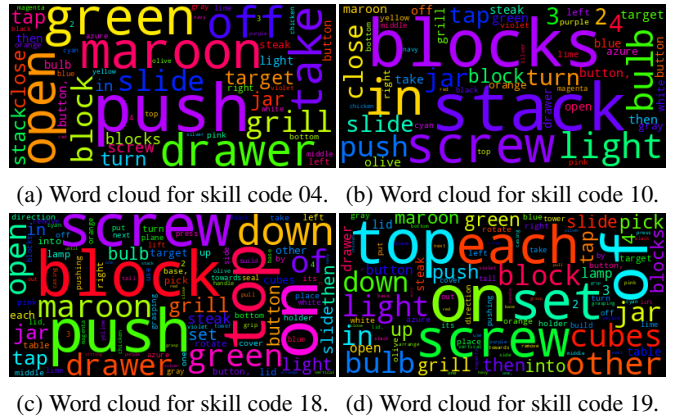


Figure 3: Word Clouds for different skill codes, with the size of each word indicating its frequency within the corresponding skill code.

Figure 3 showcases several word cloud examples corresponding to different skill codes. Upon inspection, it becomes evident that each skill code emphasizes distinct aspects of the evaluated tasks. For instance, Skill Code 04 (refer to Figure 3a) appears to hold greater significance in tasks such as “open drawer”, “meat off grill”, and “slide block”, with a notable focus on colors. Conversely, Skill Code 10 (refer to Figure 3b) is centered around tasks like “stack blocks” and “screw bulb”, placing emphasis on numerical values to indicate the quantity of objects being manipulated. Furthermore, Skill Codes 18 and 19, both associated with the action of “screw”, but exhibit unique characteristics (refer to Figures 3c and 3d). Skill Code 18 demonstrates a closer relationship to the task “slide block”, featuring words like “tap” and “jar” that denote screw-like actions, albeit without explicit mentions of “screwing”. In contrast, Skill Code 19 appears to highlight the relative positions of manipulable objects.

By examining the common tasks associated with each skill code, we can derive abstract insights into the underlying sub-actions represented by the skills. For example, Skill Code 04 could suggest a common sub-action of “grabbing an object” across tasks like “open drawer”, “meat off grill”, and “slide block”. Similarly, Skill Code 10 implies a common sub-action of “placing an object on top of another” in tasks such as “stack blocks” and “screw bulb”. However, it’s important to note that these interpretations are based on human induction, as there may be a lack of alignment between the language instructions and the delineation of key points. Future endeavors could focus on refining this process by decomposing the language instructions and correlating language fragments with demonstration snippets to generate more convincing explanations.

## 5 Conclusion and Future Work

This paper introduces Ex-PERACT, an explainable hierarchical multi-task behavior cloning agent. At the top level, Ex-PERACT learns discrete skill codes via clustering, while the bottom level utilizes skill codes, language, and observations to acquire a proficient behavioral policy by representing the problem as discrete 3D voxel grids. Our experiments on 6-DOF manipulation tasks illustrate that Ex-PERACT demonstrates promising performance compared to other baseline methods, concurrently providing an human-understandable visualization of skills learned by the agent.

However, certain limitations of Ex-PERACT persist and warrant exploration as potential future research directions. Given Ex-PERACT’s ability to accommodate various forms of language instructions, developing a model to decompose various language in-

structions to cooperate with trajectory key points could be one interesting direction to further enhance explainability. Additionally, EXPERACT faces challenges in long-term tasks and tasks characterized by high variability. Subsequent research endeavors may prioritize enhancing its performance, addressing not only the breadth of tasks but also considerations of task length and variance.

## References

- [1] M. Beliaev, A. Shih, S. Ermon, D. Sadigh, and R. Pedarsani. Imitation learning by estimating expertise of demonstrators. In *International Conference on Machine Learning*, pages 1732–1748. PMLR, 2022.
- [2] T. Bewley, J. Lawry, and A. Richards. Modelling agent policies with interpretable imitation learning. In *International Workshop on the Foundations of Trustworthy AI Integrating Learning, Optimization and Reasoning*, pages 180–186. Springer, 2020.
- [3] D. Brown, R. Coleman, R. Srinivasan, and S. Niekum. Safe imitation learning via fast bayesian-aware inference from preferences. In *International Conference on Machine Learning*, pages 1165–1177. PMLR, 2020.
- [4] D. Chen and R. Mooney. Learning to interpret natural language navigation instructions from observations. In *Proceedings of the AAAI Conference on Artificial Intelligence*, volume 25, pages 859–865, 2011.
- [5] F. Codevilla, M. Müller, A. López, V. Koltun, and A. Dosovitskiy. End-to-end driving via conditional imitation learning. In *2018 IEEE international conference on robotics and automation (ICRA)*, pages 4693–4700. IEEE, 2018.
- [6] A. Dosovitskiy, L. Beyer, A. Kolesnikov, D. Weissenborn, X. Zhai, T. Unterthiner, M. Dehghani, M. Minderer, G. Heigold, S. Gelly, et al. An image is worth 16x16 words: Transformers for image recognition at scale. *arXiv preprint arXiv:2010.11929*, 2020.
- [7] D. Garg, S. Vaidyanath, K. Kim, J. Song, and S. Ermon. Lisa: Learning interpretable skill abstractions from language. *Advances in Neural Information Processing Systems*, 35:21711–21724, 2022.
- [8] P.-L. Guhur, S. Chen, R. G. Pintel, M. Tapaswi, I. Laptev, and C. Schmid. Instruction-driven history-aware policies for robotic manipulations. In *Conference on Robot Learning*, pages 175–187. PMLR, 2023.
- [9] K. Hakhamaneshi, R. Zhao, A. Zhan, P. Abbeel, and M. Laskin. Hierarchical few-shot imitation with skill transition models. In *International Conference on Learning Representations*, 2022.
- [10] A. Jaegle, S. Borgeaud, J.-B. Alayrac, C. Doersch, C. Ionescu, D. Ding, S. Koppula, D. Zoran, A. Brock, E. Shelhamer, et al. Perceiver io: A general architecture for structured inputs & outputs. *arXiv preprint arXiv:2107.14795*, 2021.
- [11] S. James, M. Freese, and A. J. Davison. Pyrep: Bringing v-rep to deep robot learning. *arXiv preprint arXiv:1906.11176*, 2019.
- [12] S. James, Z. Ma, D. R. Arrojo, and A. J. Davison. Rlbench: The robot learning benchmark & learning environment. *IEEE Robotics and Automation Letters*, 5(2):3019–3026, 2020.
- [13] S. James, K. Wada, T. Laidlow, and A. J. Davison. Coarse-to-fine q-attention: Efficient learning for visual robotic manipulation via discretisation. In *Proceedings of the IEEE/CVF Conference on Computer Vision and Pattern Recognition*, pages 13739–13748, 2022.
- [14] E. Jang, A. Irpan, M. Khansari, D. Kappler, F. Ebert, C. Lynch, S. Levine, and C. Finn. Bc-z: Zero-shot task generalization with robotic imitation learning. In *Conference on Robot Learning*, pages 991–1002. PMLR, 2022.
- [15] Y. Jiang, W. Yu, D. Song, W. Cheng, and H. Chen. Interpretable skill learning for dynamic treatment regimes through imitation. In *2023 57th Annual Conference on Information Sciences and Systems (CISS)*, pages 1–6. IEEE, 2023.
- [16] S. Karamcheti, S. Nair, A. S. Chen, T. Kollar, C. Finn, D. Sadigh, and P. Liang. Language-driven representation learning for robotics. *arXiv preprint arXiv:2302.12766*, 2023.
- [17] H. Le, N. Jiang, A. Agarwal, M. Dudík, Y. Yue, and H. Daumé III. Hierarchical imitation and reinforcement learning. In *International conference on machine learning*, pages 2917–2926. PMLR, 2018.
- [18] T. Leech. *Explainable machine learning for task planning in robotics*. PhD thesis, Massachusetts Institute of Technology, 2019.
- [19] Y. Li, J. Song, and S. Ermon. Infogail: Interpretable imitation learning from visual demonstrations. *Advances in neural information processing systems*, 30, 2017.
- [20] C. Lynch and P. Sermanet. Language conditioned imitation learning over unstructured data. *arXiv preprint arXiv:2005.07648*, 2020.
- [21] S. Nair, E. Mitchell, K. Chen, S. Savarese, C. Finn, et al. Learning language-conditioned robot behavior from offline data and crowd-sourced annotation. In *Conference on Robot Learning*, pages 1303–1315. PMLR, 2022.
- [22] J. Oh, Y. Guo, S. Singh, and H. Lee. Self-imitation learning. In *International conference on machine learning*, pages 3878–3887. PMLR, 2018.
- [23] Y. Pan, C.-A. Cheng, K. Saigol, K. Lee, X. Yan, E. Theodorou, and B. Boots. Agile autonomous driving using end-to-end deep imitation learning. *arXiv preprint arXiv:1709.07174*, 2017.
- [24] A. Radford, J. W. Kim, C. Hallacy, A. Ramesh, G. Goh, S. Agarwal, G. Sastry, A. Askell, P. Mishkin, J. Clark, et al. Learning transferable visual models from natural language supervision. In *International conference on machine learning*, pages 8748–8763. PMLR, 2021.
- [25] J. Roh, C. Paxton, A. Pronobis, A. Farhadi, and D. Fox. Conditional driving from natural language instructions. In *Conference on Robot Learning*, pages 540–551. PMLR, 2020.
- [26] E. Rohmer, S. P. Singh, and M. Freese. V-rep: A versatile and scalable robot simulation framework. In *2013 IEEE/RSJ international conference on intelligent robots and systems*, pages 1321–1326. IEEE, 2013.
- [27] A. Sharma, M. Sharma, N. Rhinehart, and K. M. Kitani. Directed-info gail: Learning hierarchical policies from unsegmented demonstrations using directed information. *arXiv preprint arXiv:1810.01266*, 2018.
- [28] M. Shridhar, L. Manuelli, and D. Fox. Cliport: What and where pathways for robotic manipulation. In *Conference on Robot Learning*, pages 894–906. PMLR, 2022.
- [29] M. Shridhar, L. Manuelli, and D. Fox. Perceiver-actor: A multi-task transformer for robotic manipulation. In *Conference on Robot Learning*, pages 785–799. PMLR, 2023.
- [30] S. Stepputtis, J. Campbell, M. Phielipp, S. Lee, C. Baral, and H. Ben Amor. Language-conditioned imitation learning for robot manipulation tasks. *Advances in Neural Information Processing Systems*, 33:13139–13150, 2020.
- [31] A. Van Den Oord, O. Vinyals, et al. Neural discrete representation learning. *Advances in neural information processing systems*, 30, 2017.
- [32] L. Wang, R. Tang, X. He, and X. He. Hierarchical imitation learning via subgoal representation learning for dynamic treatment recommendation. In *Proceedings of the Fifteenth ACM International Conference on Web Search and Data Mining*, pages 1081–1089, 2022.
- [33] T. Xiao, H. Chan, P. Sermanet, A. Wahid, A. Brohan, K. Hausman, S. Levine, and J. Tompson. Robotic skill acquisition via instruction augmentation with vision-language models. *arXiv preprint arXiv:2211.11736*, 2022.
- [34] Y. Xie, S. Vosoughi, and S. Hassanpour. Towards interpretable deep reinforcement learning models via inverse reinforcement learning. In *2022 26th International Conference on Pattern Recognition (ICPR)*, pages 5067–5074. IEEE, 2022.
- [35] Y. You, J. Li, S. Reddi, J. Hseu, S. Kumar, S. Bhojanapalli, X. Song, J. Demmel, K. Keutzer, and C.-J. Hsieh. Large batch optimization for deep learning: Training bert in 76 minutes. *arXiv preprint arXiv:1904.00962*, 2019.
- [36] T. Yu, C. Finn, A. Xie, S. Dasari, T. Zhang, P. Abbeel, and S. Levine. One-shot imitation from observing humans via domain-adaptive meta-learning. *arXiv preprint arXiv:1802.01557*, 2018.
- [37] D. Zhang, Q. Li, Y. Zheng, L. Wei, D. Zhang, and Z. Zhang. Explainable hierarchical imitation learning for robotic drink pouring. *IEEE Transactions on Automation Science and Engineering*, 19(4):3871–3887, 2021.
- [38] Z. Zhang and I. Paschalidis. Provable hierarchical imitation learning via em. In *International Conference on Artificial Intelligence and Statistics*, pages 883–891. PMLR, 2021.
- [39] L. Zhou and K. Small. Inverse reinforcement learning with natural language goals. In *Proceedings of the AAAI Conference on Artificial Intelligence*, volume 35, pages 11116–11124, 2021.